Active vibration reduction by optimally placed sensors and actuators with application to stiffened plates by beams

Daraji, A. H. & Hale, J. M.

Original citation & hyperlink:
Daraji, AH & Hale, JM 2014, 'Active vibration reduction by optimally placed sensors and actuators with application to stiffened plates by beams' Smart Materials and Structures, vol. 23, no. 11, 115018.
https://dx.doi.org/10.1088/0964-1726/23/11/115018

DOI 10.1088/0964-1726/23/11/115018
ISSN 0964-1726
ESSN 1361-665X

Publisher: IOP Publishing

Active Vibration Reduction by Optimally Placed Sensors and Actuators with Application to Stiffened Plates by Beams

[1]A.H. Daraji and [2]J.M. Hale
[1]Electromechanical Department, University of Technology, Baghdad, Iraq
[2]School of Mechanical and Systems Engineering, Newcastle University, Newcastle, UK
[1]Email: alialdraji@yahoo.com [2]Email: jack.hale@ncl.ac.uk

Abstract

This study concerns new investigation of active vibration reduction of a stiffened plate bonded with discrete sensor/actuator pairs located optimally using genetic algorithms based on a developed finite element modelling. An isotropic plate element stiffened by a number of beam elements on its edges and having a piezoelectric sensor and actuator pair bonded to its surfaces is modelled using the finite element method and Hamilton's principle, taking into account the effects of piezoelectric mass, stiffness and electromechanical coupling. The modelling is based on the first order shear deformation theory taking into account the effects of bending, membrane and shear deformation for the plate, the stiffening beam and the piezoelectric patches. A Matlab finite element program has been built for the stiffened plate model and verified with ANSYS and also experimentally.

Optimal placement of ten piezoelectric sensor/actuator pairs and optimal feedback gain for active vibration reduction are investigated for a plate stiffened by two beams arranged in the form of a cross. The genetic algorithm was set up for optimization of sensor/actuator placement and feedback gain based on the minimization of the optimal linear quadratic index as an objective function to suppress the first six modes of vibration.

Comparison study is presented for active vibration reduction of a square cantilever plate stiffened by crossed beams with two sensor/actuator configurations: firstly, ten piezoelectric sensor/actuator pairs are located in optimal positions; secondly, a piezoelectric layer of single sensor/actuator pair covering the whole of the stiffened plate as a SISO system.

Keywords , vibration control, stiffened plate by beams , optimal placement , piezoelectric, genetic algorithm

---

1. Introduction

Active vibration control is often considered as superior to passive control, being a higher response, smarter and lighter solution to the problem of structural vibration. It requires sensors, actuators, controller and driving control energy to apply opposite strain to that occurring naturally in a flexible structure to suppress vibration. The amount of external controller energy can be substantial, and this has attracted researchers to optimise it through investigation of sensor/actuator placement and control schemes.

Modelling of smart structure with bonded distributed piezoelectric sensor/actuator pairs have been investigated thoroughly for the suppression of mechanical vibration. Lee modelled a flexible laminated plate with a distribution of piezoelectric sensor/actuators bonded to it to effect distributed control and sensing of bending, torsion, shearing, shrinking and stretching based on classical laminated thin plate theory[1]. Tzou and Tseng modelled a mechanical structure (plate/shell) with bonded distributed piezoelectric sensor/actuator pairs using the finite element method and Hamilton's principle. They proposed a new piezoelectric finite element including an internal electric degree of freedom [2].

Detwiler et al modelled a laminated composite plate containing distributed piezoelectric sensor/actuators using finite element and variational principle based on first order shear deformation theory [3]. Ha et al studied a laminated composite plate containing distributed piezoelectric ceramics using eight-node brick finite elements to investigate static and dynamic response under mechanical and electrical loading [4]. A finite element solution using Navier theory is implemented by Reddy for a composite plate with a distributed piezoelectric sensor/actuator layer subjected to both mechanical and electrical disturbance based on classical and shear deformation theory. A simple negative velocity feedback is applied to control dynamic response of the structure [5].

He et al researched plate material functionally graded in the thickness direction with distributed piezoelectric material based on classical laminated plate theory. A constant velocity feedback control scheme was applied to study dynamic response of a plate and they found that the vibration amplitude of the plate attenuated at very high rates for appropriate gain values [6]. Kumar et al studied composite plates and shells with a bonded piezoelectric sensor/actuator layer using Hamilton's principle and finite element analysis based on first order shear deformation theory including the effects of mechanical, electrical and thermal loading. Negative velocity feedback control was used for shape control and vibration suppression of a cylindrical shell [7]. Han and Lee modelled a composite plate with distributed piezoelectric actuators based on layerwise theory to include in-plane displacement through the thickness. Classical control theory was implemented to compare the results with a model based on shear deformation theory and they reported that the layerwise model was more realistic [8]. Simoes et al investigated a thin laminated structure with integral piezoelectric sensor and actuator layers based on Kirchhoff classical laminate theory and finite elements. Negative constant velocity feedback was realised to suppress vibration for a composite beam and plate [9].

Plates and shells stiffened by beams are used to construct mechanical structures with increased specific strength and stiffness and investigated extensively for modal vibration behaviour. However, only a limited number of papers have been published on research into active vibration control of plates and shells stiffened by beams. Birman and Adali studied an orthotropic plate stiffened by a row of piezoelectric actuators to improve dynamic response by applying voltage to the actuators. Displacement and velocity dynamic response are considered as quadratic cost functions. They reported that increasing actuator voltage and width of stiffener-actuators led to reduced vibration suppression time [10]. Beams, plates and cylinders stiffened by piezoelectric beams were studied by Young and Hansen theoretically and experimentally. The beam stiffener had a flange and actuators were placed between the stiffener flange and the plate, and a row of error sensors was located near the stiffener. The authors found that one row of piezoelectric stiffeners and one row of error sensors is quite enough to suppress vibration in beams and plates, but a cylinder requires three or four rows to suppress vibration. In addition, they noted that the locations of piezoelectric stiffeners and error sensors are inconvenient for many modes of vibration [11]. Mukherjee et al investigated the active vibration control of piezolaminated stiffened plates, but neglected the coupling between the direct and converse piezoelectric effects. The beam stiffener could take any direction on the plate and did not need to pass through nodal elements. Displacement and negative velocity feedback control were used to suppress vibration and they identified the problem that this tended to excite higher order modes [12]. The most recent study in this area was conducted in 2010 by Balamurugan and Narayanan, who considered active vibration control for a composite shell and plate stiffened by beams with distributed piezoelectric sensor/actuator pair bonded to its surfaces. The stiffener was positioned anywhere within the shell element along lines of natural coordinates. A number of examples was studied of cantilever stiffened plates and cylindrical shells bonded to partial and full coverage piezoelectric sensor and actuator to attenuate the first eight modes of vibration using optimal linear quadratic control. They reported that these structures with full coverage sensor and actuator did not detect vibration and actuate the structure effectively for all the modes. This was because of the elimination of sensor voltage for some modes in full coverage case [13].

The researchers [10-13] investigated plates and shells stiffened by beams with piezoelectric sensor/actuator pairs distributed over the whole surface or arbitrarily located at discrete points about the surface. However many researchers have drawn attention to the importance of discrete sensors, actuators and their location to achieve high sensing and actuating effects with low feedback voltage, high response and stability. Lim investigated vibration reduction for a clamped square plate and found that discrete piezoelectric sensor/actuator pairs in specified locations achieved higher controller effect, lower power requirement and lighter weight than fully distributed piezoelectric layers [14]. Shen and Homaifar reported active damping controllers based on the use of discrete point piezoelectric sensors and actuators [15]. Balamurugan and Narayanan found that a full cover piezoelectric sensor or actuator layer bonded on a plate stiffened by beams gives low sensing and controlling effects for all modes of vibration [13]. Kumar and Narayanan showed that misplaced sensors and actuators lead to problems such as lack of observability and controllability [16]. Kumar et al showed that controllability depends on coverage area of piezoelectric sensor/actuator and that increasing the area beyond a certain limit does not improve controllability, so that the use of piezoelectric patches near the free end of a cantilever cylindrical shell is of little use [7]. Kapuria and Yasin reported that the closed loop response exhibits faster attenuation for multi-segment electrodes than a single-segment electrode for all control laws [17]. Good controller effect and optimality is achieved by discrete piezoelectric sensors/actuators and their location on a structure. Considerable work has been published to optimise the location of piezoelectric sensors and actuators to achieve higher response, stability and controller energy for plates, shells and beams. However, optimization of location for discrete piezoelectric sensors and actuators on a plate stiffened by beams has never been investigated.

In this paper, a model was developed for isotropic plate stiffened by beams bonded with discrete sensors and actuators using the finite element method and Hamilton's principle. The model was implemented to find the optimal placement of ten piezoelectric sensor/actuator pairs for a cross-stiffened plate mounted as a cantilever, considering the effects of the first six vibration modes collectively.

2. Stiffened Plate Model

Consider a flexible plate stiffened by a number of beams with a number of piezoelectric sensor/actuator pairs bonded to it. The stiffened plate is discretised to finite elements, with each plate element having the possibility of stiffening at one or more of its edges by between zero and four beam elements, and bonded to the plate element a piezoelectric sensor/actuator pair as shown in Figure (1). It is assumed that the piezoelectric elements are bonded tightly to the plate element, that the beam stiffener elements are fixed on plate element edges, and that the piezoelectric sensor area is the same as the actuator and plate area and is not affected by the thickness of the stiffener beams. The plate, beam and piezoelectric patch is analysed according to first order shear deformation theory taking account of bending, membrane and shear strain effects.

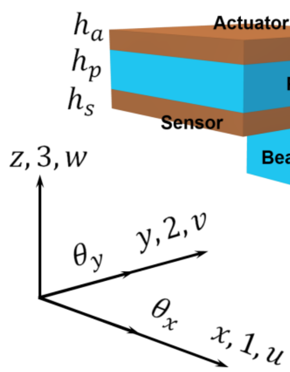

Figure1 Plate element stiffened by a beam with a piezoelectric sensor/actuator pair bonded to the surfaces

2.1 Plate element

The plate is discretised to isoparametric four nodes elements. The element displacements are a function of point coordinates and time as follows:

$$u(x, y, z, t) = u_o(x, y, t) - z\theta_x(x, y, t),$$
$$v(x, y, z, t) = v_o(x, y, t) - z\theta_y(x, y, t)\,, \tag{1}$$
$$w(x, y, z, t) = w_o\,(x, y, t)$$

$$\begin{Bmatrix} u_o \\ v_o \\ w_o \end{Bmatrix} = \sum_{i=1}^{4} N_i(s,r) \begin{Bmatrix} u_{oi} \\ v_{oi} \\ w_{oi} \end{Bmatrix}, \qquad \begin{Bmatrix} \theta_x \\ \theta_y \end{Bmatrix} = \sum_{i=1}^{4} N_i(s,r) \begin{Bmatrix} \theta_{xi} \\ \theta_{yi} \end{Bmatrix} \tag{2}$$

$$\begin{Bmatrix} x \\ y \end{Bmatrix} = \sum_{1}^{4} N_i(s,r) \begin{Bmatrix} x_i \\ y_i \end{Bmatrix} \tag{3}$$

For an isoparametric element, the element displacements and coordinates x, y are related to nodal displacements and coordinates by the same shape function $N_i(s,r)$. The shape function describes the element geometry in terms of natural coordinates s, r, which vary between -1 and 1. The strain deformation induced in a plate element is:

$$\varepsilon = \begin{Bmatrix} \dfrac{\partial u}{\partial x} \\ \dfrac{\partial v}{\partial y} \\ \dfrac{\partial u}{\partial y} + \dfrac{\partial v}{\partial x} \end{Bmatrix} = \begin{Bmatrix} \dfrac{\partial u_o}{\partial x} - z\dfrac{\partial \theta_x}{\partial x} \\ \dfrac{\partial v_o}{\partial y} - z\dfrac{\partial \theta_y}{\partial y} \\ \dfrac{\partial u_o}{\partial y} + \dfrac{\partial v_o}{\partial x} - z\left(\dfrac{\partial \theta_x}{\partial y} + \dfrac{\partial \theta_y}{\partial x}\right) \end{Bmatrix} \tag{4}$$

$$\varepsilon = \sum_{i=1}^{4} (B_{mi}\delta_i + zB_{bi}\delta_i) = B_m\delta \ + zB_b\delta \tag{5}$$

$$\gamma = \begin{Bmatrix} \dfrac{\partial w}{\partial x} - \theta_x \\ \dfrac{\partial w}{\partial y} - \theta_y \end{Bmatrix} = \sum_{i=1}^{4} B_{shi}\delta_i \ = B_{sh}\delta \tag{6}$$

Here the subscripts b, m, sh and i denote to bending, membrane, shear strain and element node number respectively.

$$B_{mi}, B_{bi}, B_{shi} = \begin{bmatrix} N_i,x & 0 & 0 & 0 & 0 \\ 0 & N_i,y & 0 & 0 & 0 \\ N_i,y & N_i,x & 0 & 0 & 0 \end{bmatrix}, \begin{bmatrix} 0 & 0 & 0 & -N_i,x & 0 \\ 0 & 0 & 0 & 0 & -N_i,y \\ 0 & 0 & 0 & -N_i,y & -N_i,x \end{bmatrix}, \begin{bmatrix} 0 & 0 & N_i,x & -N_i & 0 \\ 0 & 0 & N_i,y & 0 & -N_i \end{bmatrix} \tag{7}$$

$$\begin{bmatrix} B_b \\ B_m \\ B_{sh} \end{bmatrix} = \begin{bmatrix} [\,B_{b1} & B_{b2} & B_{b3} & B_{b4}] \\ [B_{m1} & B_{m2} & B_{m3} & B_{m4}] \\ [B_{sh1} & B_{sh2} & B_{sh3} & B_{sh4}] \end{bmatrix} \tag{8}$$

$$\delta = \{\delta_1 \quad \delta_2 \quad \delta_3 \quad \delta_4\}^T \quad , \quad \delta_i = \{u_{oi} \quad v_{oi} \quad w_{oi} \quad \theta_{xi} \quad \theta_{yi}\}^T \tag{9}$$

Here B_b , B_m and B_{sh} are bending, membrane and shear differential matrices which relate element strain to element nodal displacements, and $i = 1, 2, 3, 4$ represent the element local node numbering.

2.2 Beam stiffener in X-direction

The beam stiffener is discretised into isoparametric two nodes elements. The element displacements are a function of point coordinates and time as follows;

$$u_{bx}(x,z,t) = u_{obx}(x,t) - z * \theta_{xbx}(x,t), \qquad w_{bx}(x,z,t) = w_{obx}\,(x,t) \tag{10}$$

$$\begin{Bmatrix} u_{obx} \\ w_{obx} \end{Bmatrix} = \sum_{i=1}^{2} N_i(s) \begin{Bmatrix} u_{obxi} \\ w_{obxi} \end{Bmatrix} \;, \qquad \theta_x = \sum_{i=1}^{2} N_i(s)\,\theta_{xbxi}$$

$$N_1 = 0.5(1-s)\;, \qquad N_2 = 0.5(1+s) \tag{11}$$

$$\varepsilon_{bx} = \frac{\partial u_{obx}}{\partial x} - z\frac{\partial \theta_{xbx}}{\partial x} = \;[B_m + zB_b]\delta_{bx} \tag{12}$$

$$\gamma_{bx} = \frac{\partial w_{bx}}{\partial x} - \theta_{xbx} = B_{sh}\delta_{bx} \tag{13}$$

$$B_b = [0 \;\; 0 \;\; 0 \; -N_1,x \;\; 0 \;\; 0 \;\; 0 \;\; 0 \; -N_2,x \;\; 0\,] \tag{14}$$

$$B_m = [N_1,x \;\; 0 \;\; 0 \;\; 0 \;\; 0 \quad N_2,x \;\; 0 \;\; 0 \;\; 0 \quad 0\,] \tag{15}$$

$$B_{sh} = [0 \quad 0 \;\; N_1,x \;\; -N_1 \;\; 0 \;\; 0 \quad 0 \;\; N_2,x \;\; -N_2 \;\; 0] \tag{16}$$

$$\delta_{bx} = \{u_{obx1} \quad 0 \quad w_{obx1} \quad \theta_{xbx1} \quad 0 \quad u_{obx2} \quad 0 \quad w_{obx2} \quad \theta_{xbx2} \quad 0\}^T \tag{17}$$

2.3 Beam element connection to plate element

The beam stiffener connection to the plate has a significant role in achieving perfect structure modelling, which depends on the offset elements node points distance between plate and beam. The offset can be ignored if it is very small compared to beam length and the transfer matrix is then considered as unity. However, it requires treatment if the offset is large compared to the plate and beam dimensions. A rough estimation of the offset was used to decide whether to ignore or model its effects based on the beam length L and the offset distance between the beam and the plate mid-plane surface as follows [18]:

1. If $PB < L/100$, the offset can be safely ignored
2. If $L/100 < PB < L/5$, the offset needs to be modelled
3. If $PB > L/5$, ordinary beam, plate and shell elements should not be used. Two or three-dimensional elements should be used instead.

Consider the section shown in Figure (2) before and after deformation of a plate stiffened by one beam in the x-direction with an offset distance of PB between two nodes P and B on the mid-plane surface of the plate and beam respectively. A transformation matrix is developed to relate the degrees of freedom of the beam to those of the plate according to Figure (2). It is assumed that the global coordinates and displacements pass through the plate element. It is also assumed that there is an imaginary link connecting the two nodal points P and B. This link is considered before and after deformation in order to determine the relationship between the degrees of freedom of the displacement for the points P and B according to Figure (2) as follows:.

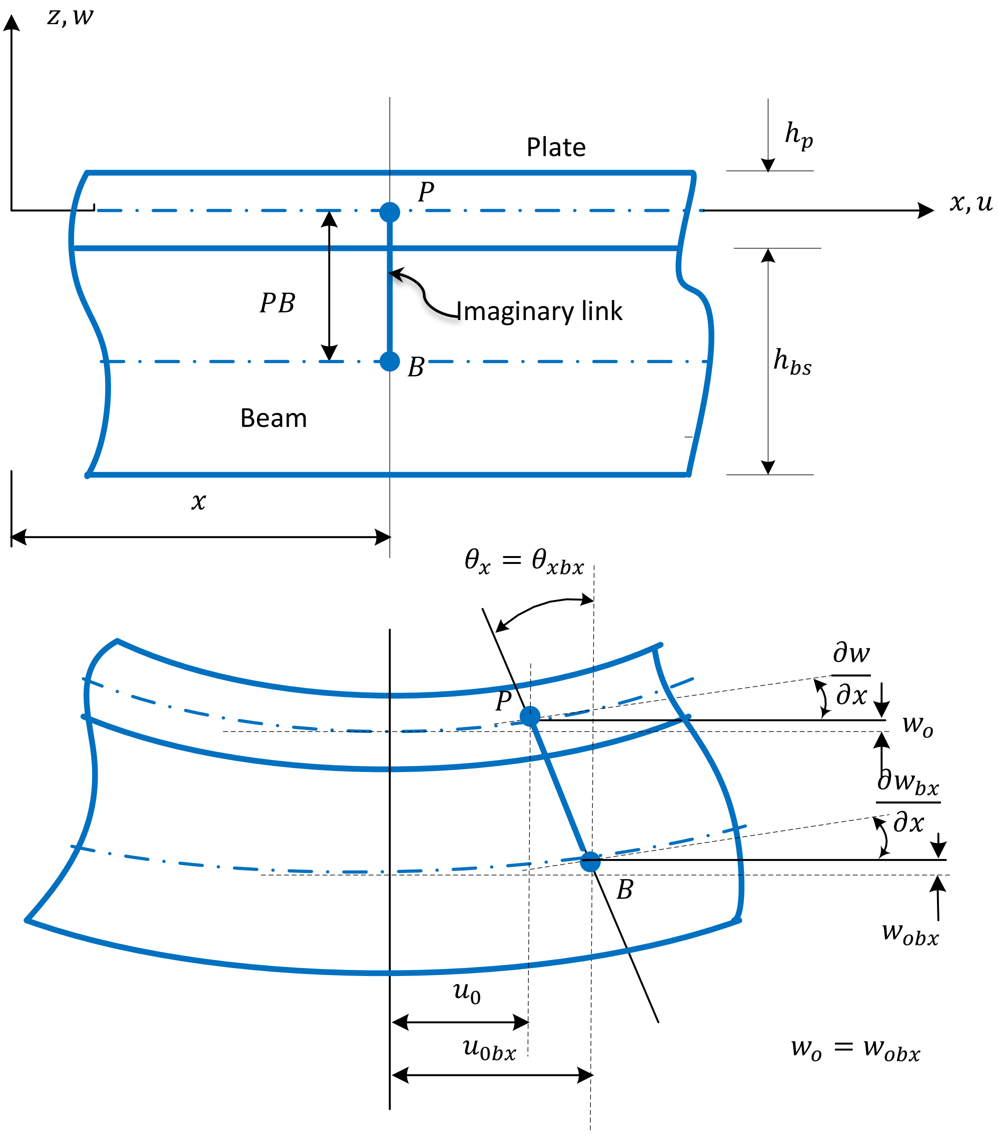

Figure 2 Section for connection of plate and beam stiffener along the x-direction before and after deformation

$$PB = 0.5(h_p + h_{bs}) \tag{18}$$

$$u_o = u_{obx} - BP * \theta_{xbx} \quad , \quad \theta_x = \theta_{xbx} \quad , \quad w_o = w_{obx} \tag{19}$$

We rearrange equation (19) in matrix form as follows:

$$\begin{Bmatrix} u_o \\ v_o \\ w_o \\ \theta_x \\ \theta_y \end{Bmatrix} = \begin{bmatrix} 1 & 0 & 0 & -BP & 0 \\ 0 & 0 & 0 & 0 & 0 \\ 0 & 0 & 1 & 0 & 0 \\ 0 & 0 & 0 & 1 & 0 \\ 0 & 0 & 0 & 0 & 0 \end{bmatrix} \begin{Bmatrix} u_{obx} \\ 0 \\ w_{obx} \\ \theta_{xbx} \\ 0 \end{Bmatrix} \tag{20}$$

$$\delta = T_x \delta_{bx} \qquad , \qquad T_x = \begin{bmatrix} T_{x1} & 0 \\ 0 & T_{x1} \end{bmatrix} \tag{21}$$

$$T_{x1} = \begin{bmatrix} 1 & 0 & 0 & -BP & 0 \\ 0 & 0 & 0 & 0 & 0 \\ 0 & 0 & 1 & 0 & 0 \\ 0 & 0 & 0 & 1 & 0 \\ 0 & 0 & 0 & 0 & 0 \end{bmatrix} \tag{22}$$

$$\delta_{bx} = T_x^{-1} \delta = T_{bx} \delta \tag{23}$$

$$\delta = \{\delta_1 \quad \delta_2\}^T \tag{24}$$

The transformation matrix for the beam stiffener in the y-direction is;

$$v_o = v_{oby} - BP * \theta_{yby} \quad , \quad \theta_y = \theta_{yby} \quad , \quad w_o = w_{oby} \tag{25}$$

$$\begin{Bmatrix} u_o \\ v_o \\ w_o \\ \theta_x \\ \theta_y \end{Bmatrix} = \begin{bmatrix} 0 & 0 & 0 & 0 & 0 \\ 0 & 1 & 0 & 0 & -BP \\ 0 & 0 & 1 & 0 & 0 \\ 0 & 0 & 0 & 0 & 0 \\ 0 & 0 & 0 & 0 & 1 \end{bmatrix} \begin{Bmatrix} 0 \\ v_{oby} \\ w_{oby} \\ 0 \\ \theta_{yby} \end{Bmatrix} \tag{26}$$

$$\delta = T_y \delta_{by} \quad , \quad T_y = \begin{bmatrix} T_{y1} & 0 \\ 0 & T_{y1} \end{bmatrix}, \qquad T_{y1} = \begin{bmatrix} 0 & 0 & 0 & 0 & 0 \\ 0 & 1 & 0 & 0 & -BP \\ 0 & 0 & 1 & 0 & 0 \\ 0 & 0 & 0 & 0 & 0 \\ 0 & 0 & 0 & 0 & 1 \end{bmatrix} \tag{27}$$

$$\delta_{by} = T_y^{-1} \delta = T_{by} \delta$$

$$\delta_{by} = \{0 \quad v_{oby1} \quad w_{oby1} \quad 0 \quad \theta_{yby1} \quad 0 \quad v_{oby2} \quad w_{oby2} \quad 0 \quad \theta_{yby2}\}^T \tag{28}$$

where T_{bx} and T_{by} are transformation matrices for the beam stiffener in the x and y-directions respectively. So, equation (23) is substituted in equations (12) and (13) to get beam element strain in terms of plate degrees of freedom.

$$\varepsilon_{bx} = [B_m + zB_b]T_{bx}\delta \quad , \quad \gamma_{bx} = B_{sh}T_{bx}\delta \tag{29}$$

2.4Piezoelectric constitutive equations

Piezoelectric materials and their applications have gradually developed since their discovery and have become a popular and essential part of control system applications. The linear constitutive equation (28) describes the coupling relationship between electrical and mechanical behaviour of piezoelectric material [19].

$$\sigma = C^E\,\varepsilon - e^T E\,,\ \ D = e\,\varepsilon + \mu^\sigma\,E \tag{30}$$

Where σ, ε, D and E are stress, strain, electrical displacement and electric field vectors respectively. C, e, and μ are elasticity, piezoelectric and permittivity matrices. Superscripts E and σ indicate that measurements are taken under constant electrical displacement and stress, respectively. Piezoelectric material coordinates 1, 2, 3 or x, y, z is shown in Figure (1). Equation (30) can be rearranged into a non-coupled form, according to the assumptions of first order shear deformation theory that the normal stress in the z-direction σ_{zz} is equal to zero and eliminating ε_{zz} by condensation. Also, the polarisation direction of piezoelectric transducer is just in the z-direction, which leads the values of D_x and D_y to be equal to zero. Substituting these values in equation (30) we obtain the following [20] .

$$\begin{Bmatrix}\sigma_{xx}\\ \sigma_{yy}\\ \tau_{xy}\end{Bmatrix} = \begin{bmatrix}\bar{C}_{11} & \bar{C}_{12} & 0\\ \bar{C}_{21} & \bar{C}_{22} & 0\\ 0 & 0 & \bar{C}_{33}\end{bmatrix}\begin{Bmatrix}\varepsilon_{xx}\\ \varepsilon_{yy}\\ \gamma_{xy}\end{Bmatrix} - \begin{bmatrix}0 & 0 & \bar{e}_{13}\\ 0 & 0 & \bar{e}_{23}\\ 0 & 0 & 0\end{bmatrix}\begin{Bmatrix}0\\ 0\\ E_z\end{Bmatrix}$$

$$\begin{Bmatrix}\tau_{yz}\\ \tau_{xz}\end{Bmatrix} = \begin{bmatrix}\bar{C}_s & 0\\ 0 & \bar{C}_s\end{bmatrix}\begin{Bmatrix}\gamma_{yz}\\ \gamma_{xz}\end{Bmatrix}$$

$$D_z = \begin{bmatrix}0 & 0 & 0\\ 0 & 0 & 0\\ \bar{e}_{13} & \bar{e}_{23} & 0\end{bmatrix}\begin{Bmatrix}\varepsilon_{xx}\\ \varepsilon_{yy}\\ \gamma_{xy}\end{Bmatrix} + \bar{\mu}^\sigma_{33}E_z$$

$$\bar{C}_{11} = C^E_{11} - \frac{{C^E_{13}}^2}{C^E_{33}} \quad , \quad \bar{C}_{12} = C^E_{12} - \frac{{C^E_{13}}^2}{C^E_{33}},$$

$$\bar{C}_{33} = \frac{C^E_{11} - C^E_{12}}{2} \quad , \quad \bar{C}_s = k(C^E_{55} - \frac{{e_{15}}^2}{\mu^\sigma_{11}})$$

$$\bar{e}_{13} = e_{31} - \frac{C^E_{13}}{C^E_{33}}e_{33} \quad , \quad \bar{e}_{23} = \bar{e}_{13} \quad , \quad \bar{\mu}^\sigma_{33} = \mu^\sigma_{33} + \frac{{e_{33}}^2}{C^E_{33}}$$

2.5 Kinetic and strain energy

Hamilton's principle and the finite element method are applied to a plate element with a bonded piezoelectric sensor/actuator pair and stiffened by a number of beams, to obtain the equilibrium dynamic equations. Hamilton's equation is:

$$\int_{t1}^{t2} \Delta(\mathcal{L} + VW)dt = \int_{t1}^{t2} \Delta\,(KE - SE + EE + VW)dt = 0 \tag{31}$$

The total kinetic energy KE in a plate element including sensor and actuator and beam stiffener is:

$$KE = KE_p + KE_s + KE_a + KE_{bs} \tag{32}$$

$$KE = 0.5\rho \int (\dot{u}_o^2 + \dot{v}_o^2 + \dot{w}_o^2 + z^2\dot{\theta}_x^2 + z^2\dot{\theta}_y^2)dzdA \tag{33}$$

$$KE = 0.5\dot{\delta}^T \left[M_p + M_a + M_s + \sum_{i=1}^{n_{bs}} M_{bsi} \right] \dot{\delta} = 0.5\dot{\delta}^T\, M_{uu}\, \dot{\delta} \tag{34}$$

$$M_p, M_a, M_s = \sum_{i=1}^{n_g}\sum_{j=1}^{n_g} N^T \Big(\rho_p \int_{-\frac{h_p}{2}}^{\frac{h_p}{2}} Z, \qquad \rho_a \int_{\frac{h_p}{2}}^{\frac{h_p}{2}+h_a} Z\,,\ \ \rho_s \int_{-\frac{h_p}{2}-h_s}^{-\frac{h_p}{2}} Z\Big)\, N\, dz\, detJ w_i w_j \tag{35}$$

$$Z = \begin{bmatrix} \bar{Z} & & & 0 \\ & \bar{Z} & & \\ & & \bar{Z} & \\ 0 & & & \bar{Z} \end{bmatrix}, \qquad \bar{Z} = \begin{bmatrix} 1 & & & & 0 \\ & 1 & & & \\ & & 1 & & \\ & 0 & & z^2 & \\ & & & & z^2 \end{bmatrix} \tag{36}$$

$$M_{bx} = 0.5\rho L_{bx} \sum_{i=1}^{n_g} T_{bx}^T\, N^T Z_{bx}\, N\, T_{bx}\, w_i \tag{37}$$

$$Z_{bx} = \begin{bmatrix} \bar{Z}_{bx} & 0 \\ 0 & \bar{Z}_{bx} \end{bmatrix}, \qquad \bar{Z}_{bx} = \begin{bmatrix} A_{bx} & & & & 0 \\ & 0 & & & \\ & & A_{bx} & & \\ & 0 & & I_{bx} & \\ & & & & 0 \end{bmatrix} \tag{38}$$

Here ng, w_i, w_j and $detJ$ denote the number of Gaussian integration, weighted points and Jacobian determinant respectively, and the subscripts, p, a and s refer to the plate, sensor and actuator respectively. The total strain energy SE induced in a plate with beam stiffeners and piezoelectric sensor/actuator pair can be described by the following equations;

$$SE = SE_p + SE_{bs} + SE_s + SE_a \tag{39}$$

$$SE_p = \frac{1}{2}\int_v \varepsilon^T \sigma \, dv_p + \frac{1}{2}\int_v \gamma^T \tau \, dv_p \tag{40}$$

$$SE_p = 0.5\delta^T \int \int_{-\frac{h_p}{2}}^{\frac{h_p}{2}} (z^2 B_b^T D_p B_b + B_m^T D_p B_m + z B_m^T D_p B_b + z B_b^T D_p B_m + B_{sh}^T D_{sh} B_{sh}) \delta dz dA \tag{41}$$

$$D_p = \frac{E}{1-\mu^2}\begin{bmatrix} 1 & \mu & 0 \\ \mu & 1 & 0 \\ 0 & 0 & \frac{1-\mu}{2} \end{bmatrix} \quad , \quad D_{sh} = \frac{kE}{2(1+\mu)}\begin{bmatrix} 1 & 0 \\ 0 & 1 \end{bmatrix} \tag{42}$$

$$\int dA = \int_{-1}^{1}\int_{-1}^{1} detJ ds dr = \sum_{i=1}^{ng}\sum_{j=1}^{ng} detJ w_i w_j \tag{43}$$

$$SE_p = 0.5\delta^T K_p \delta \tag{44}$$

Where D_p and D_{sh} denote plate bending and shear elasticity matrices. E, μ and k refer to modulus of elasticity, Poisson's ratio and shear correction factor, respectively. Strain energy induced in the beam stiffener is then:

$$SE_{bs} = 0.5\delta^T T_{bx}^T \sum_{i=1}^{ng} (B_b^T E I_{bx} B_b + B_m^T E A_{bx} B_m + 0.25 B_m^T E h A_{bx} B_b + 0.25 B_b^T E h A_{bx} B_m + B_{sh}^T \frac{kEA_{bx}}{2(1+\mu)} B_{sh}) \, T_{bx} \delta 0.5 L_{bx} w_i \tag{45}$$

$$SE_{bs} = 0.5\delta^T K_{bs} \delta \tag{46}$$

Here $T_{bx}, E,$ A_{bx} and I_{bx} refer to transformation matrix, modulus of elasticity, area and second moment of area for the beam in the x-direction. K_p and K_{bs} represent plate and beam element stiffness matrices respectively. Strain energy induced in the actuator is:

$$SE_a = \frac{1}{2}\int_v \varepsilon^T \sigma \, dv_a + \frac{1}{2}\int_v \gamma^T \tau \, dv_a \tag{47}$$

The electrical potential field distribution E_z varies linearly across the thickness of a piezoelectric element and the voltage difference across its thickness is constant over its whole area:

$$E_z = -\frac{\Delta\phi}{h} \, , \quad E_s = -\begin{Bmatrix} 0 \\ 0 \\ 1/h_s \end{Bmatrix} \phi_s = -B_\emptyset^s \phi_s \, , \qquad E_a = -\begin{Bmatrix} 0 \\ 0 \\ 1/h_a \end{Bmatrix} \phi_a = -B_\emptyset^a \phi_a \tag{48}$$

Where ϕ_s and ϕ_a are single voltage degrees of freedom over the top centre surface of sensor and actuator respectively.

$$SE_a = 0.5\delta^T \int \int_{\frac{h_p}{2}}^{\frac{h_p}{2}+h_a} ((z^2 B_b^T \bar{C} B_b + B_m^T \bar{C} B_m + z B_m^T \bar{C} B_b$$
$$+ z B_b^T \bar{C} B_m + B_{sh}^T \bar{C}_s B_{sh})\delta + z B_b^T \bar{e}^T B_\emptyset^a \phi_a + B_m^T \bar{e}^T B_\emptyset^a \phi_a) dz dA \tag{49}$$

$$SE_a = 0.5\delta^T K_{pz}^a \delta + 0.5\delta^T K_{u\emptyset}^a \phi_a \tag{50}$$

In the same way, we can obtain the strain energy induced in the sensor, represented by equation (51);

$$SE_s = 0.5\delta^T K_{pz}^s \delta + 0.5\delta^T K_{u\emptyset}^s \phi_s \tag{51}$$

Where K_{pz} and $K_{u\phi}$ refer to piezoelectric sensor/actuator stiffness and electromechanical coupling matrices respectively. Total elastic energy induced in a plate, beam stiffener and piezoelectric element are obtained by substituting equations (44), (46), (50) and (51) in equation (39), from which:

$$SE = 0.5\delta^T \left[K_p + K_{bs} + K_{pz}^a + K_{pz}^s\right]\delta + 0.5\delta^T K_{u\emptyset}^s \phi_s + 0.5\delta^T K_{u\emptyset}^a \phi_a \tag{52}$$

$$SE = 0.5\delta^T \left(K_{uu}\delta + K_{u\emptyset}^s \phi_s + K_{u\emptyset}^a \phi_a\right) \tag{53}$$

Where K_{uu} represents the total mechanical stiffness matrix for a plate, beam stiffener, and piezoelectric sensor/actuator element. Electrical energy induced in a sensor element is:

$$EE_s = \frac{1}{2}\int_v E^T D \, dv_s = \frac{1}{2}\int_v E^T (\bar{e}\,\varepsilon + \bar{\mu}_{33}^\sigma E)\, dv_s \tag{54}$$

$$EE_s = 0.5\phi_s^T \int \int_{-\frac{h_p}{2}-h_s}^{-\frac{h_p}{2}} -B_\emptyset^{s\,T} ((z\bar{e}B_b + \bar{e}B_m)\delta - \bar{\mu}_{33}^\sigma B_\emptyset^s \phi_s) dz dA \tag{55}$$

$$EE_s = -0.5\phi_s^T K_{\emptyset u}^s \delta - 0.5\phi_s^T K_{\emptyset\emptyset}^s \phi_s \tag{56}$$

In the same way, we can obtain the electrical energy induced in an actuator represented by equation (57)

$$EE_a = -0.5\phi_a^T K_{\emptyset u}^a \delta - 0.5\phi_a^T K_{\emptyset\emptyset}^a \phi_a \tag{57}$$

$K_{\phi\phi}$ is the piezoelectric capacitance matrix. The virtual work done by external mechanical and electric forces is:

$$VW = \delta^T F_u - \phi_a^T F_\phi \tag{58}$$

Where F_u and F_ϕ refer to mechanical force and applied charge respectively. Substituting equations (34), (53), (56), (57) and (58) in equation (31), we obtain equations (59)-(62):

$$M_{uu}\ddot{\delta} + \overline{K}_{uu}\delta = F_u - K^a_{u\emptyset}\phi_a \tag{59}$$

$$K^a_{\emptyset u}\delta + K^a_{\emptyset\emptyset}\,\phi_a = F_\phi \tag{60}$$

$$K^s_{\emptyset u}\delta + K^s_{\emptyset\emptyset}\phi_s = 0 \tag{61}$$

$$\overline{K}_{uu} = K_{uu} - K^s_{u\emptyset}K^s_{\emptyset\emptyset}K^s_{\emptyset u} \tag{62}$$

2.6 Global assembly

The equation (63) represents the dynamic equation for a single plate element with a bonded piezoelectric sensor/actuator pair and stiffened by a number of beam element. The plate element may have a piezoelectric sensor/actuator pair and/or a number of beam element stiffeners, or may have neither. It is necessary to assemble the global matrices of the plate including beam stiffeners and piezoelectric sensor/actuator pairs as follows:

$$M_g = \sum_{k=1}^{nel} T_k^T\, M_p T_k + \sum_{k=1}^{nsa} T_k^T\, [M_s + M_a]T_k + \sum_{n=1}^{nbs} T_n^T\, M_{bs}T_n \tag{63}$$

$$K_g = \sum_{k=1}^{nel} T_k^T\, K_p T_k + \sum_{n=1}^{nbs} T_n^T\, K_{bs}T_n + \sum_{k=1}^{nsa} T_k^T\left[K^a_{pz} + K^s_{pz} - K^s_{u\emptyset}K^s_{\emptyset\emptyset}K^s_{\emptyset u}\right]T_k \tag{64}$$

$$\bar{F}_u = \sum_{k=1}^{nel} T_k^T\, F_u \qquad , \qquad \bar{F}_\emptyset = \sum_{k=1}^{n_{sa}} T_k^T\, K^a_{u\emptyset}\phi_a \tag{65}$$

Where nel, nsa and nbs are the total number of plate, sensors/actuator pairs and beam stiffeners element respectively. M_g and K_g refer to global mass and stiffness matrices for the structure including plate, piezoelectric pairs and beams stiffener. T_k and T_n are distributed matrix defined by the following [21]:

$$T_k(i,j) = \begin{Bmatrix} 0 \; if\; j \neq m_k(i) \\ 1 \; if\; j = m_k(i) \end{Bmatrix} \qquad for \qquad \begin{matrix} i = 1,2,\ldots,20 \\ j = 1,2,\ldots,n_{gdof} \end{matrix} \tag{66}$$

$$m_{k\,(1,20)} = \{5n_k - 4 \quad 5n_k - 3 \quad 5n_k - 2 \quad 5n_k - 1 \quad 5n_k\} \tag{67}$$

$$T_n(i,j) = \begin{Bmatrix} 0 \; if\; j \neq m_n(i) \\ 1 \; if\; j = m_n(i) \end{Bmatrix} for \qquad \begin{matrix} i = 1,2,\ldots,10 \\ j = 1,2,\ldots,n_{gdof} \end{matrix} \tag{68}$$

$$m_{n\,(1,10)} = \{5n_n - 4 \quad 5n_n - 3 \quad 5n_n - 2 \quad 5n_n - 1 \quad 5n_n\} \tag{69}$$

where n_k (four nodes) is the global element nodal numbering for the plate, while beam n_n (two nodes), sensor and actuator global element nodal numbering follows the same plate nodal numbering according to their location on the plate, n_{gdof}, m_k and m_n are the global degrees of freedom, plate and beam indexing vector containing five global degree of freedom per node for k^{th} and n^{th} number of elements node respectively. So, the global dynamic equation for the plate stiffened by number of beam stiffeners and bonded by number of discrete piezoelectric sensor/actuator pairs may be written in the following form:

$$M_g \ddot{\delta} + C\dot{\delta} + K_g \delta = \bar{F}_u - \bar{F}_\emptyset \tag{70}$$

2.7 Modal equation

Low modes of vibration are difficult and costly to analyse using equation (70). So, superposition is realised by transferring the number of coupled equations from displacement in physical coordinates to the same number of uncoupled equations in terms of modal displacement coordinates, which makes it easier to investigate the contribution of each mode individually. The general dynamic equation in terms of modal displacement coordinates is a powerful equation to describe the motion of the system in each individual mode. The orthogonal properties of mass and stiffness are;

$$\varphi^T M \varphi = I \quad , \quad \varphi^T K \varphi = \Omega \, , \quad \varphi^T C \varphi = 2\xi\omega \tag{71}$$

The relation between physical and modal displacements is represented by the following equation:

$$\delta = \varphi\, \eta \quad , \quad \dot{\delta} = \varphi\, \dot{\eta} \quad , \quad \ddot{\delta} = \varphi\, \ddot{\eta} \tag{72}$$

Where δ and η are displacement in physical and modal coordinates respectively, φ and Ω refer to mode shape and natural frequency matrices. Substituting equations (71) and (72) in (70) we obtain a modal non-coupled dynamic equation:

$$\ddot{\eta} \;+\; 2\xi\omega\dot{\eta} + \;\Omega\, \eta = \varphi^T\, F_u - \varphi^T K_{u\emptyset}^a \phi_a \tag{73}$$

$$\phi_s = -\varphi^T {K_{\emptyset\emptyset}^s}^{-1}\, K_{\emptyset u}^s \eta \tag{74}$$

In order to put equations (73) and (74) into state space form and to change them from second order to a linear first order equation, assume that:

$$X = \begin{Bmatrix} X_1 \\ X_2 \end{Bmatrix} = \begin{Bmatrix} \eta \\ \dot{\eta} \end{Bmatrix} \quad , \quad \dot{X} = \begin{Bmatrix} \dot{X}_1 \\ \dot{X}_2 \end{Bmatrix} = \begin{Bmatrix} \dot{\eta} \\ \ddot{\eta} \end{Bmatrix} \tag{75}$$

$$\dot{X} = \begin{bmatrix} 0 & \omega \\ -\omega & -2\xi\omega \end{bmatrix} X + \begin{bmatrix} 0 \\ \varphi^T \end{bmatrix} F_d + \begin{bmatrix} 0 \\ -\varphi^T K_{u\emptyset}^a \end{bmatrix} \phi_a \tag{76}$$

$$\dot{X} = AX + B\phi_a + B_{md} F_d \quad , \quad \phi_s = C_i\, X_i \tag{77}$$

$$A_i = \begin{bmatrix} 0 & \omega_i \\ -\omega_i & -2\xi_i\omega_i \end{bmatrix} \quad , \quad B_i = \begin{bmatrix} 0 \\ -\varphi^T K_{u\emptyset}^a \end{bmatrix} , \qquad B_{mdi} = \begin{bmatrix} 0 \\ \varphi^T \end{bmatrix}$$

$$C_i = \begin{bmatrix} -\varphi^T \omega_i^{-1} \, K_{\emptyset\emptyset}^{s\;-1} K_{u\emptyset}^s & 0 \end{bmatrix} \quad , \qquad X_i = \{\omega_i\eta_i \quad \dot{\eta}_i\}^T \tag{78}$$

Where A_i , B_i , B_{di} and C_i are individual modal state and input actuator, disturbance and output sensor matrices respectively in which subscript *i* refers to mode number. The state matrices for a number of modes n_m and number of actuators r_a are:

$$A_{(2n_m \times 2n_m)} = \begin{bmatrix} A_1 & \cdots & 0 \\ \vdots & \ddots & \vdots \\ 0 & \cdots & A_{n_m} \end{bmatrix} \tag{79}$$

$$B_{(2n_m \times r_a)} = \begin{bmatrix} (B_1)_1 & \cdots & (B_1)_{r_a} \\ \vdots & \cdots & \vdots \\ (B_{n_m})_1 & \cdots & (B_{n_m})_{r_a} \end{bmatrix} \tag{80}$$

$$C_{(r_a \times 2n_m)} = \begin{bmatrix} (C_1)_1 & \cdots & (C_{n_m})_1 \\ \vdots & \cdots & \vdots \\ (C_1)_{r_a} & \cdots & (C_{n_m})_{r_a} \end{bmatrix} \tag{81}$$

$$X_{(2n_m \times 1)} = \{\omega_1\eta_1 \quad \dot{\eta}_1 \quad \cdots \quad \omega_{n_m}\eta_{n_m} \quad \dot{\eta}_{n_m}\}^T \tag{82}$$

It is shown in the literature relevant to the active vibration reduction of stiffened plates explained in section 1 that the optimisation of the location of discrete piezoelectric transducers on a plate stiffened by beams has never been modelled and investigated. In this study, the contribution of this finite element model is that it is able to solve and optimise the locations, feedback gain and number of discrete sensors and actuators for unstiffened plates and those stiffened by beams passing through the plate's finite element nodes in any configuration in order to optimise active vibration reduction for these structures.

3. Control Law and Objective Function

Linear quadratic optimal controller design is based on minimization of performance index *J*. Values of positive-definite weighted matrices Q, of dimension $(2n_m \times 2n_m)$, and R of dimension $(r_a \times r_a)$ are controlled by the value of the performance index, where n_m, r_a represent the number of modes and actuators, respectively. These matrices are established by the relative importance of error and controller energy, with high values of Q giving high vibration suppression. Optimal control system design for a given linear system is realised by minimization of performance index *J*.

$$J = \int_0^{\infty} (X^T Q X \ \ + u^{\,T} R\, u\,) dt \tag{83}$$

$$J = \int_0^{\infty} X^T [Q + \mathrm{K^T} R \mathrm{K}] X dt \tag{84}$$

Ogata has shown it is possible to follow this derivation to design a linear quadratic controller, which leads to the following Riccati equation[22]:

$$A^T P + PA - PBR^{-1} B^T P + Q = 0 \tag{85}$$

$$K = R^{-1} B^T P\,, \qquad\qquad u = -\mathrm{KX} \tag{86}$$

Solution of the Reduced Riccati equation (85) gives the value of matrix P; if matrix P is positive definite then the system is stable or the closed loop matrix $A - BK$ is stable. Feedback control gain can be obtained after substitution of P in equation (86). Minimization of the linear quadratic cost function J is taken as an objective function to optimise gain and piezoelectric actuator locations [23]. It can be seen from the Riccati equation (85) that the Riccati solution matrix P is a function of actuator location matrix B while the matrices R, Q and A are constant for a particular control system. The linear quadratic cost function J is equal to the trace P. The minimum value of P gives optimal B piezoelectric actuator location and minimum feedback gain K. So:

$$J(x, y) = Trace\big(P(x, y)\big) \tag{86}$$

$$J_{opt}(x, y) = \min(Trace\big(P(x, y)\big), K\,) \tag{87}$$

Where $x, y\ \in$ plate dimension $500 \times\ 500$ mm

4. Genetic algorithm

In 1975, Holland invented the genetic algorithm, a heuristic method based on “survival of the fittest” or the principle of natural evolution. It has been continuously improved and is now a powerful method for searching optimal solutions. An Optimization problem consists of a large number of possible solutions called the search space, each of which can be marked by a fitness value depending on a problem definition or fitness function. An exhaustive search, in which every element of the search space is evaluated, is very costly. For example, the work described here involves the optimal location of ten sensor/actuator pairs in a plate discretised into 100 elements, so the size of the search space is the statistical combination of 10 items from 100, or 1.73×10^{13} possible solutions. The genetic algorithm gives an efficient search method for the global optimal solution and is largely immune to the problem of becoming “stuck” in a local optimum.

The fundamental unit in the genetic algorithm is a population of individuals, each defined by a chromosome containing a number of genes. The effectiveness or “fitness” of each individual is calculated according to some rule using the values of the genes. The members of the population with the highest fitness values are allowed to “breed” to form the next generation and the process continues until convergence is achieved. In this case, the ten “genes” are the locations of the ten sensor/actuator pairs, defined by an integer number (1-100), and the fitness function is the linear quadratic index.

This process is directly analogous to the survival of the fittest concept in Darwinian natural selection, in which the more successful individuals in a population are inclined to breed and so form the next generation. By this means the genes that code for desirable characteristics, and so give the individuals possessing them a high degree of fitness, are transmitted down the generations at the expense of less useful genes, which die out.

The working mechanism of the genetic algorithm is represented by two stages: firstly selection of the breeding population from the current whole population, and secondly reproduction. The process is started by defining a population of individuals at random from the search space, the chromosome of each being made up of ten random numbers in the range 1-100, representing the locations of the ten sensor/actuator pairs on the plate. This is the population of the first generation. In the selection process, the fitness function value for each individual is calculated using these genetic values as data, and the breeding population defined as those with the highest value of fitness function. The reproduction process is closely based on sexual reproduction. Pairs of individuals from the breeding population share their genetic material to produce offspring containing a combination of their parents’ genes.

Many strategies have been developed for the reproduction process, but all involve “crossover” and mutation. In crossover, the chromosome of each parent is broken and two new chromosomes formed from the pieces. In mutation, one or more genes in a child’s chromosome are changed randomly. In this way crossover explores the known regions of the search space by testing different combinations of genes that have been shown to promote high fitness, while mutation helps to maintain diversity in the population and so explore new regions of the search space.. The process continues for many generations until the population converges on a single optimal solution, which is to say that the chromosomes of all members of the breeding population are almost identical.

In this work, a genetic algorithm program was written in Matlab m-code. Its main features are:

1. Suitable values of $\mathrm{Q} = 10 \times 10^{11} \times \mathrm{I}_{2\mathrm{n_m},2\mathrm{n_m}}$ and $\mathrm{R} = \mathrm{I}_{\mathrm{r_a},\mathrm{r_a}}$ are set by the user.
2. The state matrix A of dimension $(2n_m, 2n_m)$ is prepared for the first six modes of vibration according to the equation (79).
3. One hundred chromosomes are chosen randomly from the search space to form the initial population.
4. The input (actuators) matrix is calculated for each chromosome and for the first six modes of vibration according to equation (80).
5. A fitness value is calculated for each member of the population based on the fitness function, according to equation (86), and stored in the chromosome string to save future recalculation.
6. The chromosomes are sorted according to their fitness value and the half with the lowest fitness values (i.e. the most fit) are selected to form the breeding population, called parents. The remaining, less fit, chromosomes are discarded.
7. The members of the breeding population are paired up in order of fitness and crossover applied to each pair, the crossover point being selected randomly and is different for each pair. This gives two new offspring (child) chromosomes with new properties.
8. A mutation rate of 5% is used on the child chromosomes.
9. The input (actuators) matrix is calculated for each child chromosome according to equation (80) and thereafter the process is repeated from 5 for a preset number of generations.

5. Results and Discussion

5.1 Problem description

A cantilever flat plate was stiffened by two beams arranged in cross configuration as shown in Figure 2. This beam stiffener configuration provides a symmetrical geometry. The plate dimensions were $500 \times 500 \times 1.9$ mm and the beam stiffener $500 \times 20 \times 1.9$ mm. Optimal placement of ten piezoelectric actuators is investigated for the stiffened plate to suppress the first six modes of vibrations using the genetic algorithm. In this paper, the genetic algorithm search space of the stiffened plate has 1.73×10^{13} candidates (solutions), one of which is the global optimum and many are local optimal solutions. The plate and piezoelectric specifications are given in Table 1.

Table 1 Plate stiffener and piezoelectric material properties

Properties	Plate	Stiffener	Piezoelectric PIC255
Modulus, GPa	210	210	-------
Density, Kg/m^3	7810	7810	7810
Poisson's ratio	0.3	0.3	-------
Thickness, mm	1.9	1.9	0.5
Length, width, mm	500, 500	500, 20	50, 50
e_{31}, e_{32} , C/m^2	---------	---------	-7.15
C_{11}^E, C_{12}^E , C_{33}^E GPa	--------	--------	123,76.7, 97.11
μ_{33}^{σ}(F/m)	--------	--------	$1.5x10^{-8}$

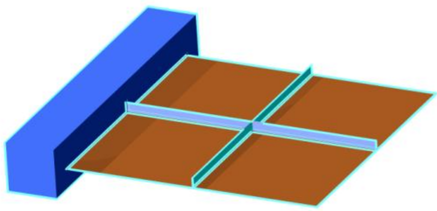

Figure 2 Cantilever plate stiffened by two beams in cross configuration with distributed piezoelectric sensor/actuator pairs bonded to the surfaces

5.2 Natural frequencies

The dynamic behaviour of the stiffened plate was investigated using the model described in section 2, and validated by the ANSYS package and experimentally. A finite element program in Matlab m-code has been built to solve for natural frequencies and mode shapes for the stiffened plate by beams, based on the model described in section 2.

The stiffened plate is represented using two dimensional SHELL63 elements and three dimensional SOLID45 elements, respectively, and the results are close to the Matlab program results as shown in Table 2. The correctness of the natural frequencies was tested by convergence to constant values with mesh refining. It has been observed that the 10×10 mesh of SHELL63 elements gave good accuracy for the first six natural frequencies compared with finer meshes, with three dimensional SOLID45 elements and compared with experimental results as shown Table 2.

The experimental validation was performed using a cross-stiffened steel plate, mounted vertically as a cantilever as shown in Figure 3 by clamping along the bottom edge. It was excited by an impact hammer to obtain the natural frequencies of vibration and modal damping ratios. The vibration was measured using a single accelerometer located at a point of large displacement in all modes. The acceleration signal was conditioned using a Kistler charge amplifier and logged using a National Instruments USB-6215 data acquisition unit and lap-top computer running LabVIEW software**.** Figure 4 shows typical experimental results in linear and logarithmic (dB) form. Modal damping, required for use with the state space matrix for optimal piezoelectric placement and vibration reduction, were calculated from the frequency response using the half-power bandwidth method. The frequency difference $\Delta\omega$ between the half power (-3dB) points on each modal peak ω_n was measured and the damping ratio calculated as $\Delta\omega/2\omega_n$. The results of experimental damping are also shown in Table 2.

Table 2 Natural Frequencies for the stiffened plate

Case	Mode					
	1^{st}	2^{nd}	3^{td}	4^{th}	5^{th}	6^{th}
Ansys Shell63 (2×2)	17.11	25.89	56.75	69.81	99.51	130.47
Ansys Shell63 (4×4)	16.75	24.55	58.59	72.16	126.05	133.89
Ansys Shell63 (10×10)	16.59	24.19	57.84	70.33	121.11	133.51
Ansys Shell63 (20×20)	16.53	24.12	57.68	70.02	120.04	132.88
Ansys Solid45 (50×50)	16.62	25.46	57.84	71.02	125.11	133.36
Present model (20×20)	15.90	25.32	56.96	70.62	125.35	132.16
Experimental	15.10	19.70	58.50	66.90	120.00	128.40
Modal damping ratio	0.032	0.0177	0.011	0.0057	0.0052	0.0022

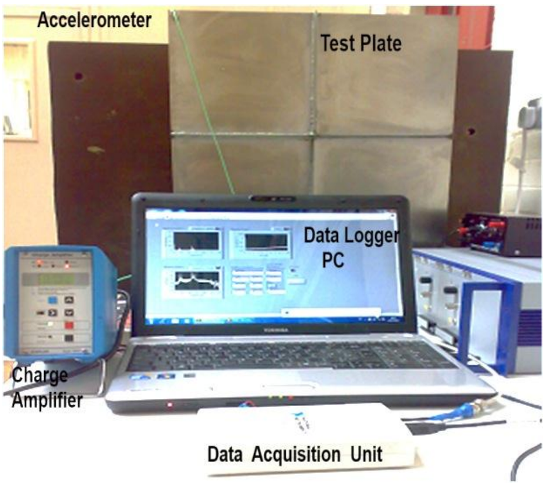

Figure 3 Test rig showing vertically mounted cantilever plate with cross stiffeners

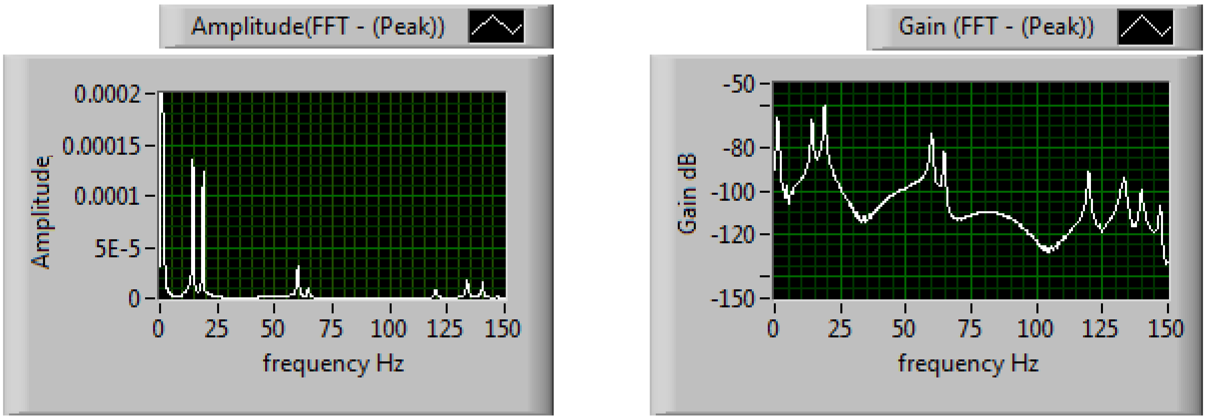

Figure 4 Experimental Lab VIEW graphs showing amplitude and frequency response for the stiffened plate

5.3 Optimization of sensor/actuator location

The genetic algorithm described in section 4 was used to find optimal locations for ten sensor/actuator pairs on 0.5m square cantilever plate with cross stiffeners. The progressive convergence of the population onto an optimal solution is shown in Figures 5a, 6a and 7a, in which the population is distributed around the circle with radius representing its fitness value to be minimised. At the first generation (Figure 5a) the population is very diverse with representatives of high and low fitness and the range in between. After fifty generations (Figure 6a) the population is much less diverse, made up of individuals of high, though not yet optimal, fitness. After 500 generations (Figure 7a) the population has almost converged to a level of fitness higher than any individual in the first or 50th generations.

This convergence is shown in another form in Figures 5b, 6b and 7b. Each point represents the location of a sensor/actuator pair for one of the individuals in a particular generation. In the first generation these locations are widely distributed, having been selected at random. After 50 generations they have begun to cluster in a few locations and after 500 generations the clustering is almost complete with all individual chromosomes coding for sensor/actuator pairs at the most ten effective sites, plus a few less effective sites distributed around the plate. It can be seen from Figures (7b and 8) that the optimal piezoelectric actuator locations are symmetrically distributed about the x-axis, which is the only axis of symmetry for the plate fixed along the left hand edge.

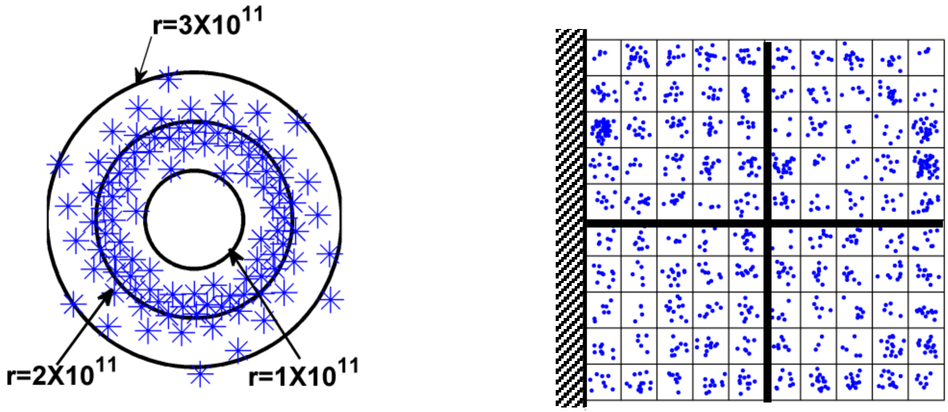

(a) Chromosomes fitness **(b) Genes distribution**

Figure 5 The first random population shown by (a) chromosome fitness and (b) distribution of genes (sensor/actuator locations) on the stiffened cantilever plate surface, **r** refers to circle radius which is the fitness value.

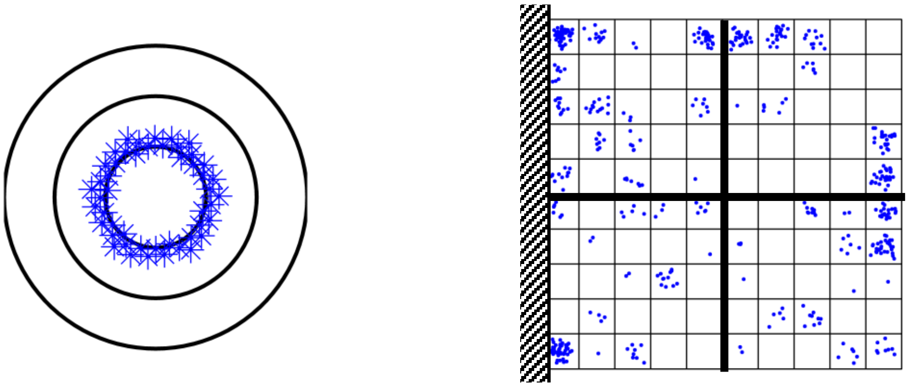

(a) Chromosomes fitness **(b) Genes distribution**

Figure 6. Population distribution after 50 generations.

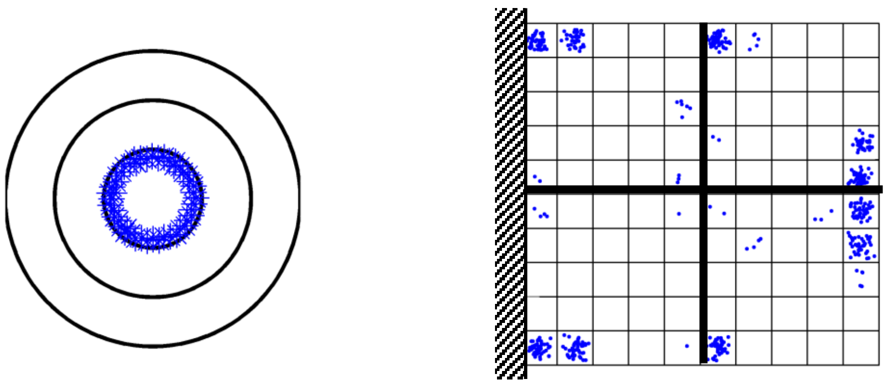

(a) Chromosomes fitness **(b) Genes distribution**

Figure 7 Population distribution after five hundred generations

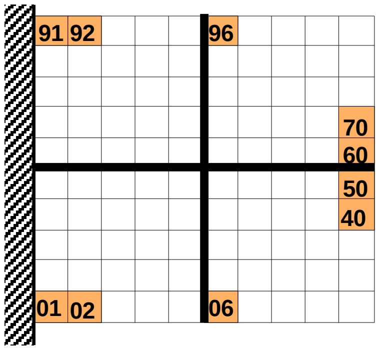

Figure 8 Optimal distribution of ten piezoelectric pairs on the stiffened cantilever plate mounted rigidly from the left hand edge

5.4 Validation of location optimization

5.4.1 *Validation by convergence*

The genetic algorithm program was run multiple times to test the repeatability of the optimised sensor/actuator locations. The results are shown in Figure 9, which gives an indication of the progress of each of five runs by plotting the fitness value for the fittest member of the breeding population at each generation. It can be seen that the final fitness value is the same in each case, though the path by which it is reached is different for each run. This indicates that the process is robust in finding the optimal solution repeatedly.

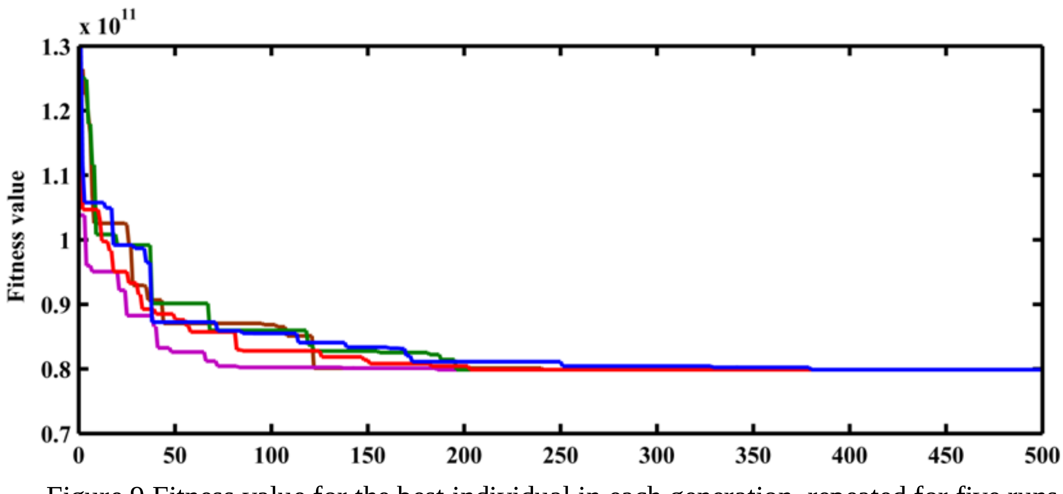

Figure 9 Fitness value for the best individual in each generation, repeated for five runs

5.4.2 Piezoelectric mass and stiffness effects

Adding piezoelectric sensor and actuator layers to the plate has two passive effects: adding stiffness and adding mass. These will both affect the natural frequencies, tending to increase and reduce them, respectively. This effect was represented using ANSYS using three dimensional SOLID45 elements for the main structure and SOLID5 elements for the piezoelectric pairs. Trials were conducted on the cross stiffened plate for three cases: no piezoelectric components; single sensor/actuator pair, giving complete coverage of both surfaces of the plate; and 10 sensor/actuator pairs in the optimal locations.

The configurations were tested and the results are shown in Table 3. It may be seen that these have a small but significant effect, but there is no simple relationship between these added layers and change in natural frequency of the various modes. These results are used in the analysis of vibration reduction for both piezoelectric configurations described in section 5.4.3.

Table (3) piezoelectric mass and stiffness effects on natural frequencies

Solid45/solid5 elements	Mode					
	1^{st}	2^{nd}	3^{td}	4^{th}	5^{th}	6^{th}
Neglecting effects	16.6	25.4	57.8	71.0	125.1	133.3
Full coverage	17.6	22.3	62.5	73.5	114.0	142.3
10 s/a pairs optimal	17.1	25.1	59.7	73.6	122.0	135.7

5.4.5 Time response ANSYS test

The effectiveness of the optimal sensor/actuator locations was investigated for the cross-type cantilever stiffened plate. The open and closed loop time responses were tested using two separate sensor/actuator configurations: the optimal configuration of ten sensor/actuator pairs as shown in Figure (10) (a), and “full coverage” with a single sensor/actuator pair covering the whole surfaces of the stiffened plate as shown in Figure (b). The plates are actuated with an out of plane sinusoidal concentrated force of constant amplitude at the free-end plate corner, and the responses are measured at the location of maximum amplitude at the other side of the free-end plate corner, sensors and actuators, as shown in Figure (10). The plates were connected to the proportional differential control scheme and represented in the ANSYS package using the APDL program.

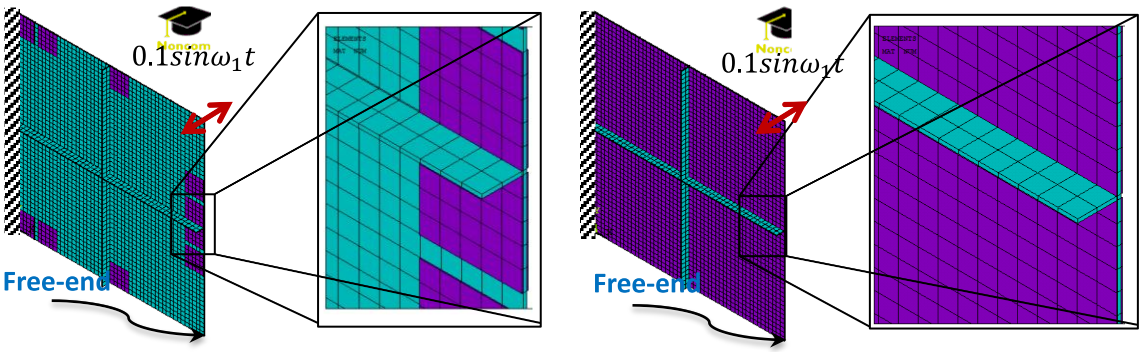

Figure 10 (**a**) Cantilever stiffened plate cross-type bonded with ten discrete sensor/actuator pairs in the optimal locations, and (**b**) single sensor/actuator cover whole the stiffened plate

The results of the open and closed loop time responses at the first mode are shown in Figure 11 (a and b) for the two configurations. Figure 11 (a1, a2, a3, a4, and a5) shows the open and closed loop time responses for the first case bonded with ten pairs in the optimal locations. Figure (11) shows that the open loop maximum vibration amplitude for the full coverage stiffened plate was lower than that for the first case as shown in Figure 11 (b3) and Figure 11 (a3) respectively. This is because the piezoelectric sensor and actuator full coverage layers increases the stiffness and structural damping of the stiffened plate.

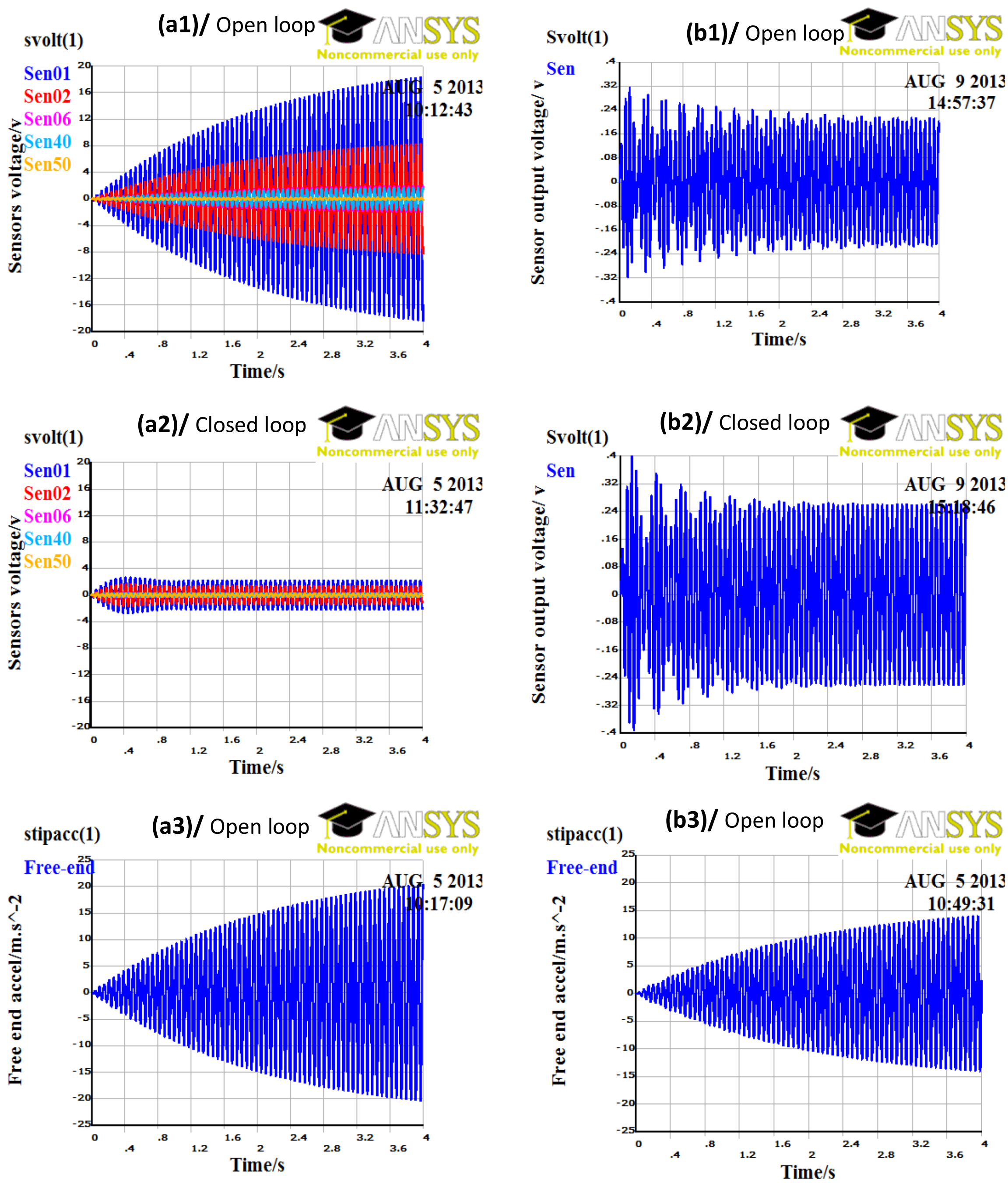

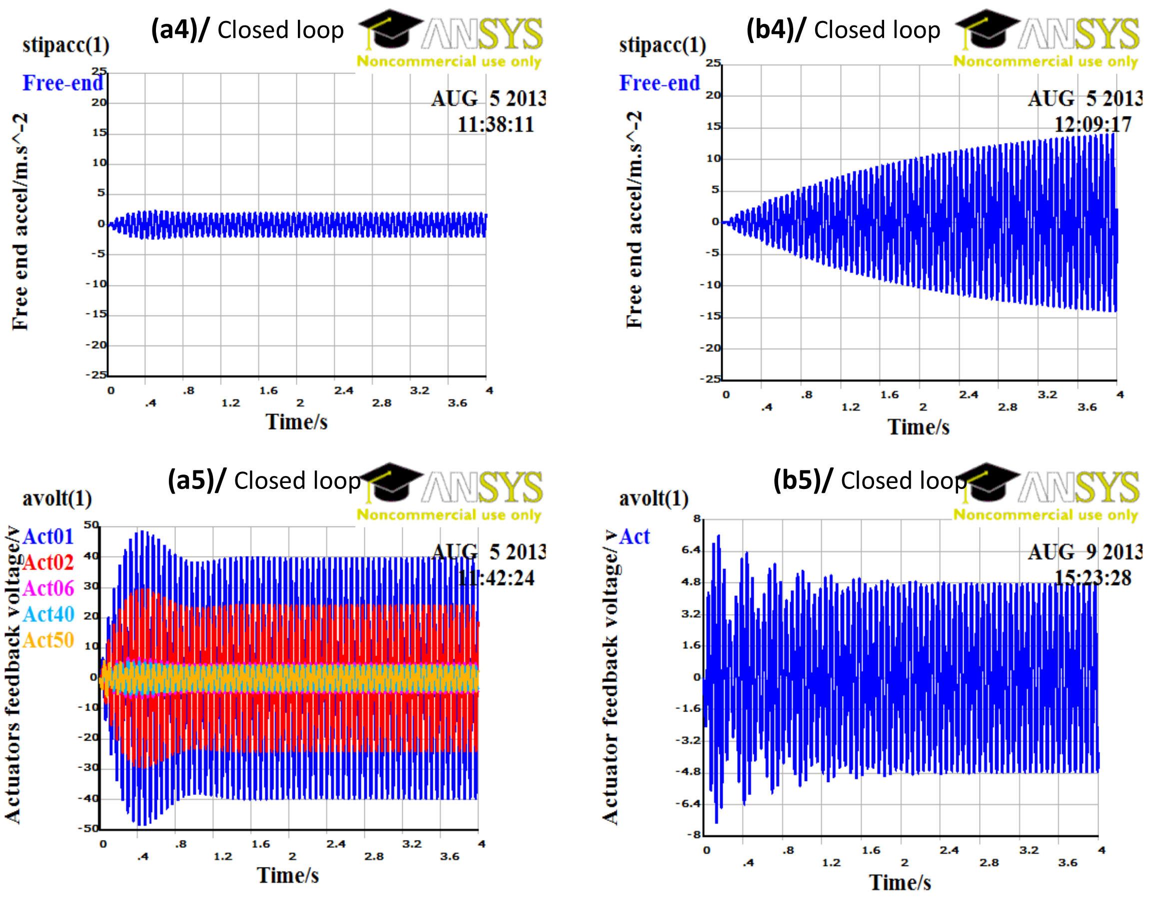

Figure 11 Open and closed loop time responses at the first mode for the cantilever stiffened plate cross-type bonded with (**a**), ten sensor/actuator pairs in the optimal locations and (**b**), single pair cover whole the stiffened plate, respectively using feedback gain $K_p = 18,\ K_d = 9$

The closed loop sensor voltage and free-end plate amplitude was reduced by 90% with total actuators (10 actuators) feedback voltage of 160V as shown in Figure 11 (a1, a2, a3, a4 and a5), no reduction was obtained in the second full coverage case, as shown in Figure 11 (b1, b2, b3, b4, and b5). It was shown that the extra increase in feedback gain led to unstable responses for full coverage case, as shown in Figure 11 (b2), where the maximum closed loop sensor voltage at steady state is larger than that for the open loop shown in Figure 11 (b1).

The results of the open and closed loop time responses at the third mode are shown in Figure 12 (a and b) for the two piezoelectric configurations. The closed loop sensor voltage and free-end amplitude responses were also reduced by 90% with a total feedback voltage 70V for the first case, as shown in Figure 12 (a1, a2, a3, a4 and a5) and no reduction at the second full coverage case as shown in Figure 12 (b1, b2, b3, b4 and b5). Unstable closed loop responses were shown at gain values $K_p = 18,\ K_d = 9$, and then the gain was reduced to $K_p = 12,\ K_d = 6$ during the test of full coverage case. In the full coverage test, no detection of vibration or actuation was found and the closed loop responses moved to unstable area at higher gain. The results of the large vibration reduction and stability obtained for the case of the optimal distribution of ten piezoelectric pairs proved the effectiveness and correctness of the placement strategy and the global optimal configurations of sensor/actuator pairs.

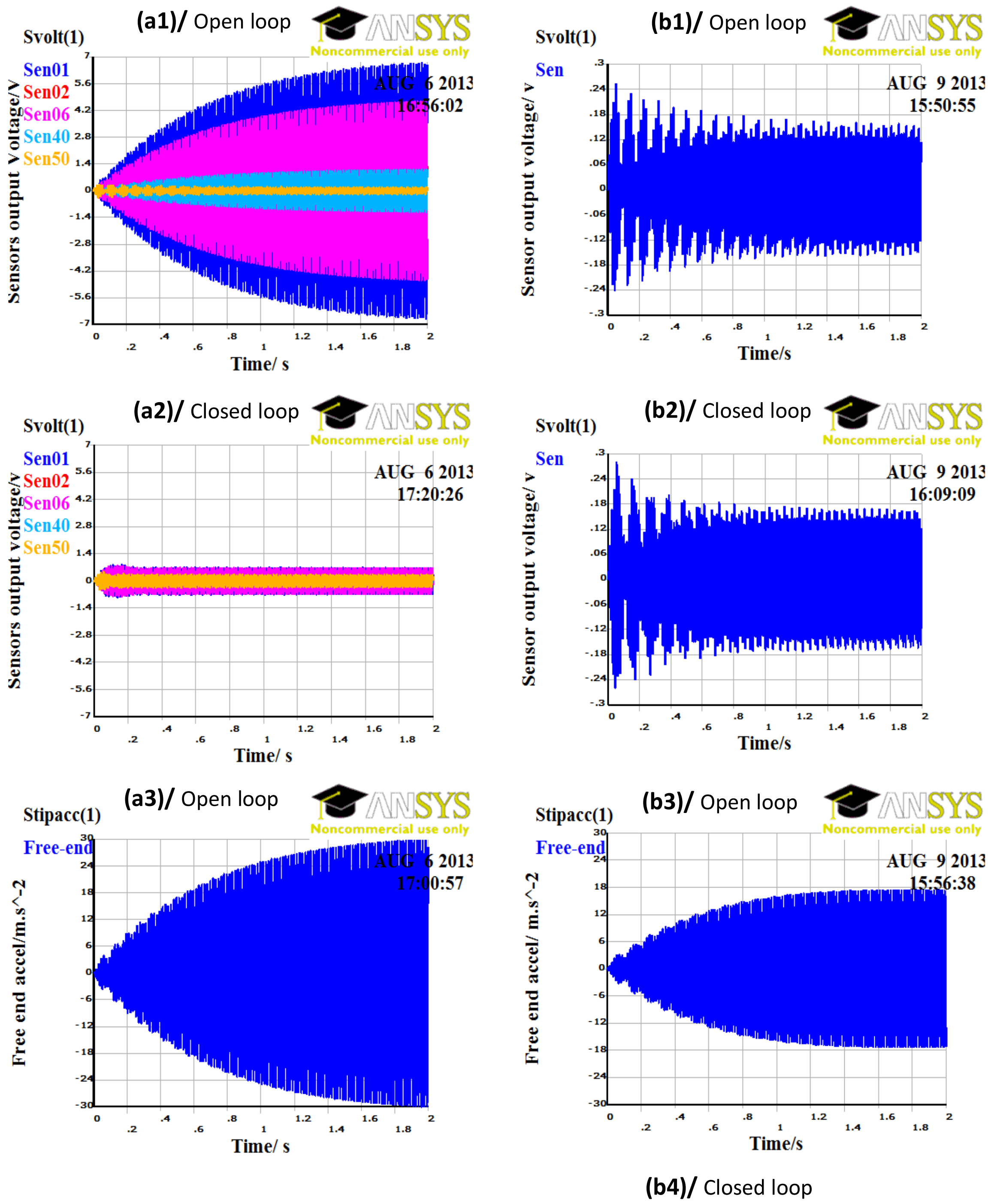

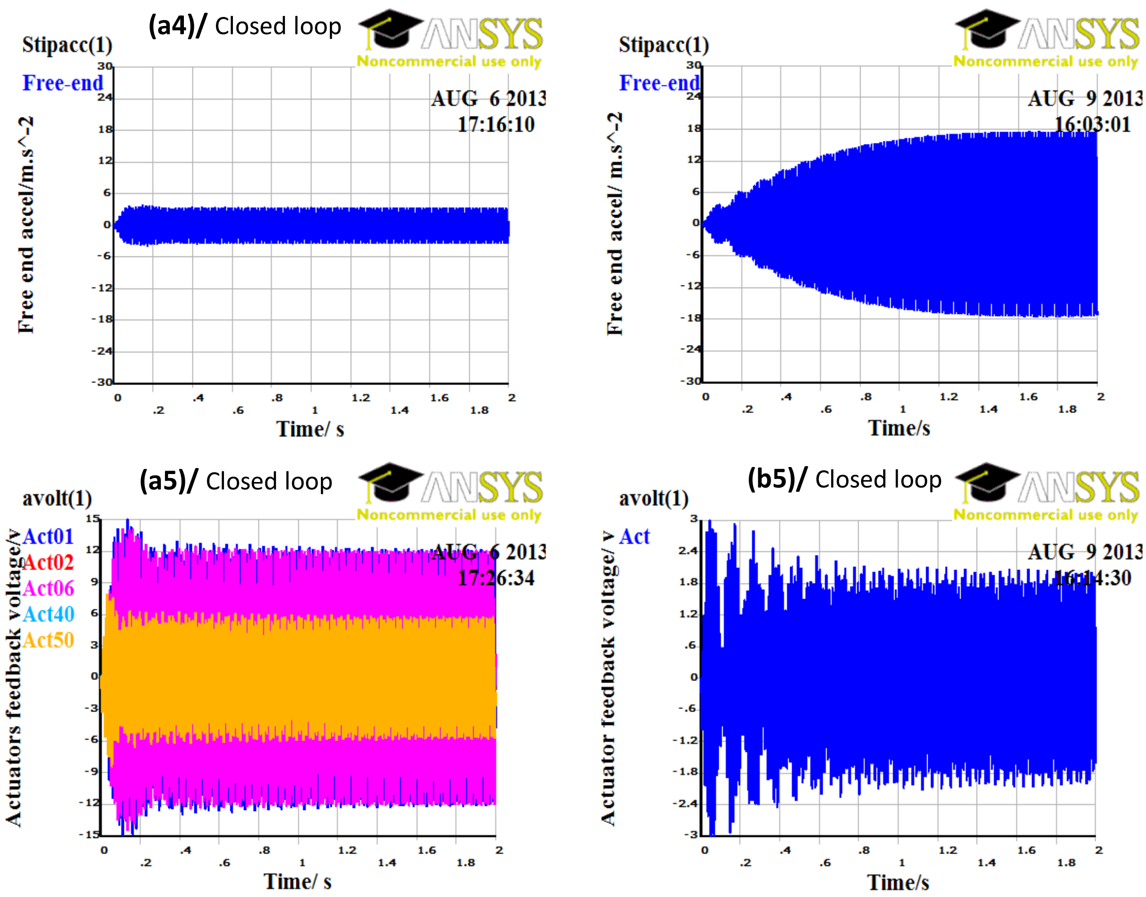

Figure 12. Open and closed loop time responses at the third mode for the cantilever stiffened plate cross-type bonded with (**a**),ten sensor/actuator pairs in the optimal locations feedback gain $K_p = 18$, $K_d = 9$ and (**b**),single pair cover whole the stiffened plate, respectively using feedback gain $K_p = 12$, $K_d = 6$

Table 4 shows the results of the comparison study of the first six modes of vibration. The results show that the closed loop time responses of vibration amplitude of the first six modes were reduced by 90% for the optimal configurations and no reduction for the full coverage piezoelectric case except the second mode was reduced by 85%.

Table 4 comparison study of vibration reduction between optimal and full coverage piezoelectric distribution

Case	1st	2nd	3th	4th	5th	6th	stability
Optimal configuration	90.9%	90.4%	90%	94.9%	90%	91%	Stable
Full coverage	0.0%	85.2%	0.0%	0.0%	0.0%	0.0%	Unstable

Conclusion

An isotropic plate stiffened by beams with bonded piezoelectric sensor actuator pairs is modelled using finite element and Hamilton's principle based on first order shear deformation theory taking account of the effects of bending, membrane and shear deformation effects for the plate, the beams and the piezoelectric patches.

A Matlab m-code finite element program has been developed to test the model and the results verified using ANSYS and experimentally.

A technique has been developed to determine optimal conditions for active vibration control of complex structures using a genetic algorithm. The parameters optimised are sensor/actuator locations and feedback gain using minimisation of linear quadratic index as the objective function. This was used to optimise the placement of ten sensor/actuator pairs from 1.73×10^{13} possible locations to give the best vibration reduction of the first six vibration modes.

The genetic algorithm optimisation was tested on a structure of moderate complexity: a cantilever mounted plate stiffened by two beams in the form of a cross. The solutions obtained were tested for robustness by running the program repeatedly. It was found that the same optimal locations were obtained in every case, following different evolutionary paths.

The effectiveness of the optimisation was tested by comparison of automatic vibration control of the cross stiffened plate using ten optimally placed sensors/actuator pairs and single sensor/actuator pair covering the whole plate surface. Vibration was reduced by more than 90% for optimal piezoelectric configuration with high stability and no reduction and stability for full coverage case except the second mode was reduced by 85%. This reflects the importance of this investigation during achievement of high vibration reduction, stability, material cost and structural weight comparing with previous studies for full coverage stiffened structures.

References

[1] Lee, C.K., *Theory of laminated piezoelectric plates for the design of distributed sensors/actuators. Part I: Governing equations and reciprocal relationships.* Journal of the Acoustical Society of America, 1990. **87**(3): p. 1144-1158.

[2] Tzou, H.S. and C.I. Tseng, *Distributed piezoelectric sensor/actuator design for dynamic measurement/control of distributed parameter systems: A piezoelectric finite element approach.* Journal of Sound and Vibration, 1990. **138**(1): p. 17-34.

[3] Detwiler, D.T., M.H.H. Shen, and V.B. Venkayya, *Finite element analysis of laminated composite structures containing distributed piezoelectric actuators and sensors.* Finite Elements in Analysis and Design, 1995. **20**(2): p. 87-100.

[4] Ha, S.K., C. Keilers, and F.-K. Chang, *Finite element analysis of composite structures containing distributed piezoceramic sensors and actuators.* AIAA journal, 1992. **30**(3): p. 772-780.

[5] Reddy, J.N., *On laminated composite plates with integrated sensors and actuators.* Engineering Structures, 1999. **21**(7): p. 568-593.

[6] He, X.Q., et al., *Active control of FGM plates with integrated piezoelectric sensors and actuators.* International Journal of Solids and Structures, 2001. **38**(9): p. 1641-1655.

[7] Kumar, R., B.K. Mishra, and S.C. Jain, *Static and dynamic analysis of smart cylindrical shell.* Finite Elements in Analysis and Design, 2008. **45**(1): p. 13-24.

[8] Han, J.-H. and I. Lee, *Analysis of composite plates with piezoelectric actuators for vibration control using layerwise displacement theory.* Composites Part B: Engineering, 1998. **29**(5): p. 621-632.

[9] Simões Moita, J.M., et al., *Active control of adaptive laminated structures with bonded piezoelectric sensors and actuators.* Computers & Structures, 2004. **82**(17-19): p. 1349-1358.

[10] Birman, V. and S. Adali, *Vibration damping using piezoelectric stiffener-actuators with application to orthotropic plates.* Composite Structures, 1996. **35**(3): p. 251-261.

[11] Young, A.J. and C.H. Hansen, *Control of flexural vibration in stiffened structures using multiple piezoceramic actuators.* Applied Acoustics, 1996. **49**(1): p. 17-48.

[12] Mukherjee, A., S.P. Joshi, and A. Ganguli, *Active vibration control of piezolaminated stiffened plates.* Composite Structures, 2002. **55**(4): p. 435-443.

[13] Balamurugan, V. and S. Narayanan, *Finite element modeling of stiffened piezolaminated plates and shells with piezoelectric layers for active vibration control.* Smart Materials and Structures. **19**(10).

[14] Lim, Y.H., *Finite-element simulation of closed loop vibration control of a smart plate under transient loading.* Smart Materials and Structures, 2003. **12**(2): p. 272-286.

[15] Shen, Y. and A. Homaifar, *Vibration control of flexible structures with PZT sensors and actuators.* JVC/Journal of Vibration and Control, 2001. **7**(3): p. 417-451.

[16] Kumar, K.R. and S. Narayanan, *The optimal location of piezoelectric actuators and sensors for vibration control of plates.* Smart Materials and Structures, 2007. **16**(6): p. 2680-2691.

[17] Kapuria, S. and M. Yaqoob Yasin, *Active vibration control of piezoelectric laminated beams with electroded actuators and sensors using an efficient finite element involving an electric node.* Smart Materials and Structures, 2010. **19**(4).

[18] Liu, G.R. and S.S. Quek, *The Finite Element Method* 1st ed. 2003, Oxford: Butterworth-Heinemann.

[19] Tiersten, H.F., *Linear Piezoelectric Plate Vibrations* 1969, New York: Plenum press

[20] Marinkovic, D., *A New Finite Composite Shell Element for Piezoelectric Active Structures* 2007, Germany: VDI Verlog Gmbh-Dusseldort.

[21] De Abreu, G.L.C.M., J.F. Ribeiro, and V. Steffen Jr, *Finite element modeling of a plate with localized piezoelectric sensors and actuators.* Journal of the Brazilian Society of Mechanical Sciences and Engineering, 2004. **26**(2): p. 117-128

[22] Ogata, K., *Modern Control Engineering*. 3td ed. 1997, London: Prentice-Hall.

[23] Kondoh, S., C. Yatomi, and K. Inoue, *Positioning of sensors and actuators in the vibration control of flexible systems.* JSME international journal, 1990. **33**(2): p. 145-152.